COMMERCIAL DEMONSTRATION OF THE NOXSO SO_2/NO_x REMOVAL FLUE GAS CLEANUP SYSTEM

Contract No. DE-FC22-91PC90549

Quarterly Technical Progress Report No. 13

Submitted to

U.S. Department of Energy
Pittsburgh Energy Technology Center

March 1, 1994 through May 31, 1994

Project Definition Phase

U.S. DOE Patent Clearance Is Not Required Prior to the Publication of this Document

DISCLAIMER

Prepared by

Morrison Knudsen Corporation
Ferguson Division
1500 West 3rd Street
Cleveland, Ohio 44113-1406

Table of Contents

List of Figures

List of Tables

EXECUTIVE SUMMARY

The NOXSO process is a dry, post-combustion flue gas treatment technology which uses a regenerable sorbent to simultaneously adsorb sulfur dioxide (SO_2) and nitrogen oxides (NO_x) from the flue gas of a coal-fired utility boiler. In the process, the SO_2 is converted to a sulfur by-product (elemental sulfur, sulfuric acid, or liquid SO_2) and the NO_x is converted to nitrogen and oxygen. It is predicted that the process can economically remove 90% of the acid rain precursor gases from the flue gas stream in a retrofit or new facility.

The objective of the NOXSO Demonstration Project is to design, construct, and operate a flue gas treatment system utilizing the NOXSO process. The effectiveness of the process will be demonstrated by achieving significant reductions in emissions of sulfur and nitrogen oxides. In addition, sufficient operating data will be obtained to confirm the process economics and provide a basis to guarantee performance on a commercial scale.

The project is presently in the project definition and preliminary design phase. Data obtained during pilot plant testing which was completed on July 30, 1993 is being incorporated in the design of the commercial size plant. A suitable host site to demonstrate the NOXSO process on a commercial scale is presently being sought.

Preliminary engineering activities involved evaluating various design options for the major process vessels with the principal focus being on the sorbent heater vessel, which is operated at the highest temperature. Additionally, the impact of the NOXSO system on power plant particulate emissions and opacity was estimated. It is predicted that particulate emissions will decrease slightly while opacity will increase slightly. Neither change will be significant enough to have an impact on emissions compliance. Advertised performance of the proposed adsorber separator is being verified by laboratory testing.

Process studies activities included POC equipment inspection and materials evaluations. Prior to demolition of the POC, visual inspections were made and samples were collected. The materials selected for the POC construction held up very well during the duration of the test program. The adsorber computer model was modified to more accurately predict the NO_x removal efficiency. Using the adsorber model as a basis, a regenerator model is being developed. Some initial runs indicate the model can reasonably predict the experimental data. The NOXSO process computer simulation has been modified to include recent design changes. Water adsorption isotherms for the NOXSO sorbent have been measured in the laboratory and are now used in calculating the sorbent heater and sorbent cooler energy balances in the process simulator. Fluid flow modeling studies are being conducted to assure that an adequate acceleration zone is provided above the top bed in all of the fluidized bed vessels.

1 INTRODUCTION

The NOXSO process is a dry, post-combustion flue gas treatment technology which uses a regenerable sorbent to simultaneously adsorb sulfur dioxide (SO_2) and nitrogen oxides (NO_x) from the flue gas of a coal-fired utility boiler. In the process, the SO_2 is converted to a sulfur by-product (elemental sulfur, sulfuric acid, or liquid SO_2) and the NO_x is reduced to nitrogen and oxygen. It is predicted that the process can economically remove 90% of the acid rain precursor gases from the flue gas stream in a retrofit or new facility.

Details of the NOXSO process are described with the aid of Figure 1-1 . Flue gas from the power plant is drawn through a flue gas booster fan which forces the air through a two-stage fluid-bed adsorber and centrifugal separator before passing to the power plant stack. Water is sprayed directly into the fluid beds as required to lower the temperature to 250-275°F by evaporative cooling. The fluid-bed adsorber contains active NOXSO sorbent. The NOXSO sorbent is a 1.6 mm diameter stabilized γ-alumina bead impregnated with 5.2 weight percent sodium. The centrifugal separator separates sorbent which may be entrained in the flue gas and returns it to the inlet of the dense phase transport system.

Spent sorbent from the adsorber flows into a dense-phase conveying system which lifts the sorbent to the top bed of the sorbent heater vessel. The sorbent flows through the multi-stage fluidized bed sorbent heater in counterflow to the heating gas which heats the sorbent to the regeneration temperature of approximately 1150°F.

In heating the sorbent, the NO_x is driven off and carried to the power plant boiler in the NO_x recycle stream. The NO_x recycle stream is cooled from approximately 450°F to 150°F in the feedwater heater. This heat-exchanger heats a slip stream of the power plant's feedwater, thereby reducing the amount of extraction steam taken from the low pressure turbine, enabling the generation of additional electricity. The cooled NO_x recycle stream replaces a portion of the combustion air. The presence of NO_x in the combustion air suppresses the formation of NO_x in the boiler resulting in a net destruction of NO_x.

The heated sorbent enters the regenerator where it is contacted with natural gas. Through a series of chemical reactions, the sulfur on the sorbent combines with the methane and forms SO_2 and H_2S. Additional regeneration occurs in the steam treater section of the regenerator when the sorbent is contacted with steam, converting the remaining sulfur on the sorbent to H_2S.

The regenerator off-gas stream is directed to a sulfur recovery plant where the H_2S and SO_2 are converted to a sulfur by-product. Elemental sulfur, sulfuric acid, and liquid SO_2 are all potential end products from the regenerator off-gas stream. Tail gas from the sulfur recovery plant will be incinerated and recycled back through the adsorbers to remove any residual sulfur compounds.

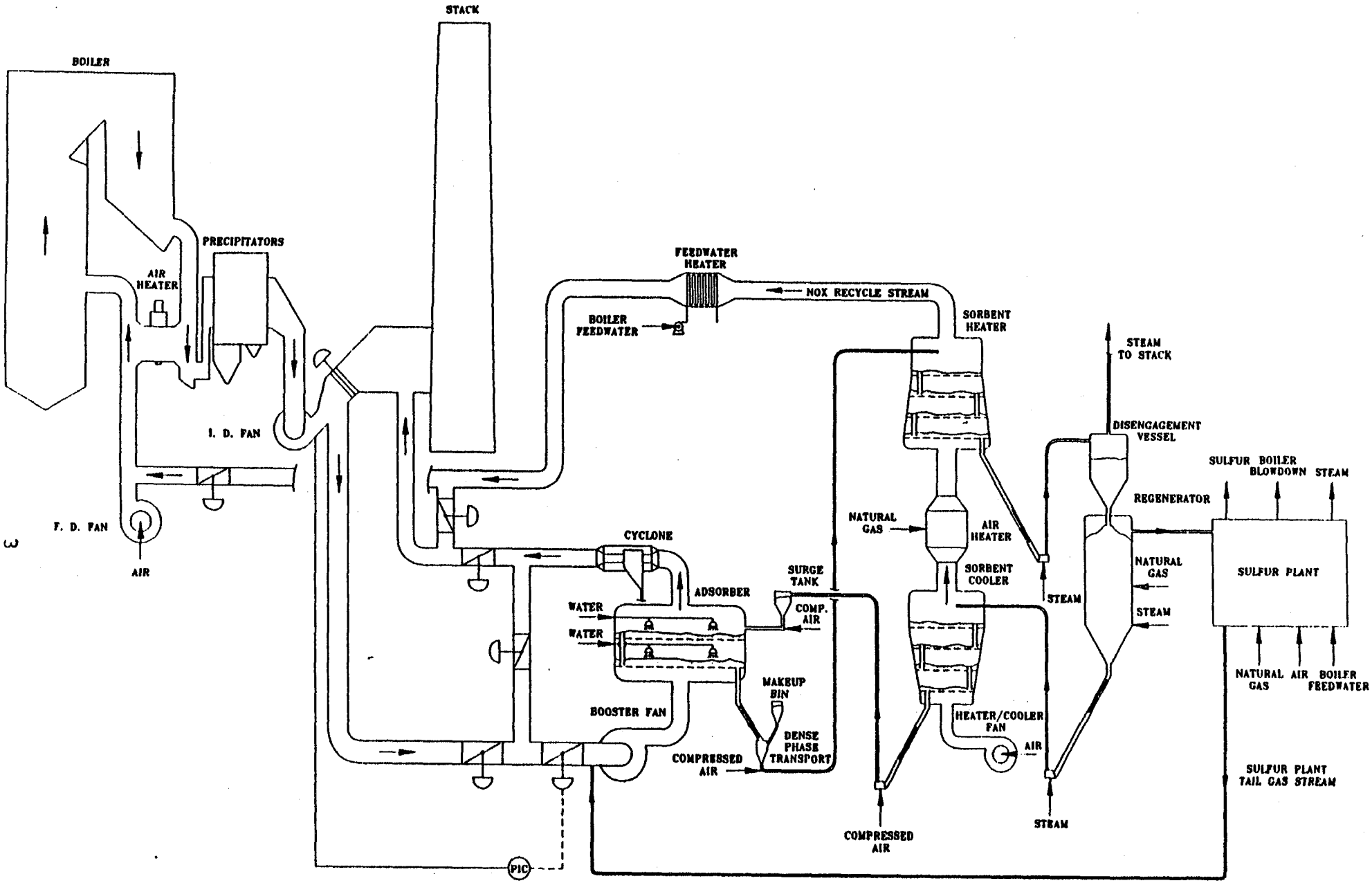

Figure 1-1. NOXSO Process Diagram

High temperature sorbent exiting the regenerator is conveyed to the multi-stage fluidized bed sorbent cooler. The sorbent flows counter to the ambient air which cools the sorbent. Regenerated sorbent exits the cooler at 300°F. It is then conveyed to the adsorber, completing the sorbent cycle.

Ambient air which is forced through the sorbent cooler by the heater-cooler fan exits the sorbent cooler at approximately 850°F. This preheated air then enters the air heater where it is heated to approximately 1325°F so it is capable of heating the sorbent exiting the sorbent heater to 1150°F.

2 PROJECT DESCRIPTION

The objective of the NOXSO Demonstration Project is to design, construct, and operate a commercial scale flue gas treatment system utilizing the NOXSO process. The effectiveness of the process will be demonstrated by achieving significant reductions in emissions of sulfur and nitrogen oxides. In addition, sufficient operating data will be obtained to confirm the process economics and provide a basis to guarantee performance on a commercial scale.

3 PROJECT STATUS

The project is currently in the project definition and preliminary design phase. This phase of the project was included to allow completion of the pilot plant testing before a significant design effort was expended. The NOXSO pilot plant test program was completed on July 30, 1993. Performance at the pilot plant exceeded the initial expectations for pollutant removal efficiency, sorbent attrition, and electrical power and natural gas consumption. Pollutant removal efficiency was enhanced significantly by the addition of the second bed in the adsorber and in bed water sprays to lower the adsorber temperature.

Data from the pilot plant has been incorporated into a fully integrated computer simulation which efficiently performs heat and material balances for the combined NOXSO plant, power plant, and sulfur plant system. The computer program also calculates sizes and capacities for the major process equipment. This computer simulation is used to evaluate process alternatives to determine their impact on process economics.

A preliminary process flow diagram and associated heat and material balances have been prepared for a commercial size plant. This flow diagram incorporates lessons learned from the pilot plant test program as well as results of laboratory process studies, theoretical process studies, and the computer simulation. Preliminary piping and instrumentation diagrams have been prepared for a commercial size plant based on the pilot plant experience and the preliminary process flow diagram.

A general arrangement has been prepared which incorporates plant design practices developed for the fluidized catalytic cracking (FCC) industry. Specifically, this design utilizes self supporting vessels, supported by skirts which extend from the vessel base to the foundation.

In contrast, the POC design utilized a tower of structural steel on which the process vessels were installed.

The search for a host site continues. Negotiations and technical evaluations of the NOXSO technology are ongoing with two potential project hosts who have signed letters of intent. Additionally, discussions with other potential hosts are at a more preliminary stage, and are not being aggressively pursued pending a final decision by the two primary candidates.

3.1 Project Management

All project management reports have been submitted to the DOE detailing project status, schedule, costs, and labor. Comparisons of planned and actual quantities were also submitted. A meeting with DOE, NOXSO, and MK-Ferguson personnel to discuss recent changes with the NEPA Process. Negotiations continue to transfer the cooperative agreement from MK-Ferguson to NOXSO Corporation. Demolition of the pilot plant is nearly complete.

3.2 NEPA Compliance

A meeting was held to discuss modifications to the process for satisfying NEPA. No other activities were conducted this quarter. As soon as a new host site is identified, the EIV draft which was prepared previously will be updated.

3.3 Preliminary Engineering

3.3.1 Sorbent Heater Vessel Design

The regenerator and steam disengaging vessels are the only process vessels that require an ASME code stamp. Because of the code stamp, these vessels must be designed according to the ASME Boiler and Pressure Vessel Code. In actual practice, all NOXSO process vessels are designed in accordance with the rules of the ASME code.

The process vessels represent a significant portion of a NOXSO plant. To minimize costs, design pressures and temperatures must be evaluated carefully. In the case of the sorbent heater, positive internal design pressure is based on the dead head pressure of the air fan plus a margin of safety to prevent lifting of the safety relief valve should the fan be dead headed. Negative internal (or external) design pressure is based on the maximum draft that the stack is capable of pulling, plus a margin of safety to prevent opening the vacuum breakers. The design temperature is set by the sorbent regeneration temperature of 1150°F. To reach this sorbent temperature requires a sorbent heater gas inlet temperature of 1325°F. To provide a margin of safety, the sorbent heater design temperature is set at 1400°F.

The design temperature and pressures dictate the vessel materials of construction and wall thicknesses. The high temperature environment requires a stainless steel shell while the pressure requirements establish the wall thickness at 1.0 to 1.5 inches, as calculated using the ASME code. A vessel of this size and thickness will have a considerable effect on cost and weight, thus

alternatives must be reviewed before finalizing this design. One such alternative being reviewed is the possibility of designing a refractory lined sorbent heater vessel. As in the case of the regenerator, the lining would be both corrosion resistant and insulating allowing the pressure boundary to be carbon steel. The shell would then be able to be thinner due to the lining which would allow the pressure boundary to be designed at a much lower temperature, thereby increasing the maximum allowable stress in the shell.

Either way, the sorbent heater will be a skirt supported vessel. The attachment point for the skirt is selected to minimize bending movements in the vessel wall and supporting skirt resulting in a predominantly compressive load. The skirt is designed using the same code rules used for the vessel under the compressive load of its own weight. Specifically, to minimize high local stress concentrations, the skirt attachment point and vessel head type are important. The ASME code suggests the use of 2:1 ellipsoidal heads with the mean diameter of the skirt coinciding with the mean diameter of the vessel. This is most important in the sorbent heater where local stress concentrations can lead to excessive creep and premature failure of the vessel.

Skirt support is desirable as opposed to lug supports due to the localized effects of each method. Hanging vessels of the weight of the sorbent heater using mounting lugs exerts large bending moments on the vessel wall. To keep vessel wall stresses within allowable limits, the walls must be thickened to accommodate the additional loading. To distribute the load exerted by the lugs, circumferential rings are attached to the lugs and vessel wall. Consequently, the additional material required for the supporting skirt is substantially off-set by elimination of the mounting lugs, thickened vessel walls, and circumferential rings.

The configuration of the sorbent heater will connect the 2:1 ellipsoidal heads with a shell that is cylindrical between the heads and the grids and conical between the grids themselves, as shown in Figure 3-1. The conical section ensures that the gas superficial velocity is constant through each of the vessel stages, thus in the sorbent heater the bottom grid will have a larger diameter than the top grid, in accordance with the gas temperature which decreases from stage to stage.

Support of the grids within the vessel also presents an important design consideration. For instance, the bottom grid is the largest and heaviest grid in the sorbent heater. It is also subjected to the highest operating temperatures and greatest sorbent load, thus, attaching this grid to the local vessel wall could produce extreme localized stresses, excessive creep, and premature failure. One option currently being considered to avoid this is an arrangement which would allow the grids to hang from a support system mounted in the cooler cylindrical area above the top grid, as shown in the left half of Figure 3-1. The grid design itself will allow for differential thermal expansion, thus minimizing any effect on the local vessel wall.

All process vessel code calculations are in a spreadsheet format for flexibility in making changes, as each NOXSO plant will be designed according to site specific conditions.

Figure 3-1. Preliminary Sorbent Heater Configuration

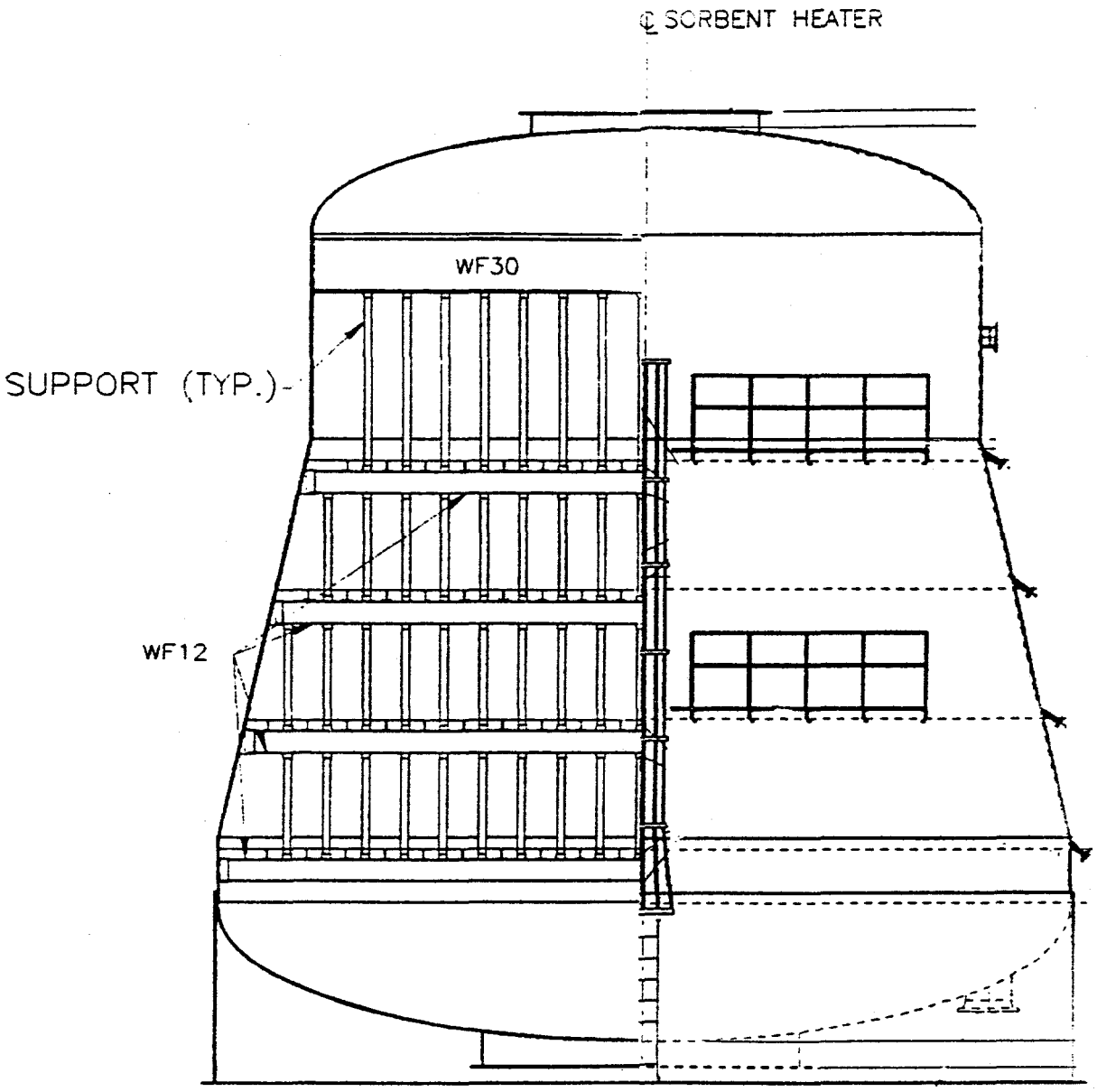

3.3.2 Particulate Emissions and Opacity

Recent efforts in preliminary engineering have investigated concerns of the impact of the integration of a NOXSO system on the host plant's particulate emissions and stack plume opacity. These concerns are genuine, as a typical NOXSO installation (100-500 MW) will experience sorbent attrition in the range of hundreds of pounds per hour. While most of this sorbent dust will end up in the boiler bottom ash, via the sorbent heater and the NO_x recycle loop, some dust will invariably be emitted through the plant stack. Current regulations for pre NSPS plants generally require particulate emissions not to exceed 0.1 lb/mmBtu while plume opacity is not to exceed 20% visibility, or a Ringelmann Number of 1. Based on the analysis summarized below, it is concluded that a power plant with a NOXSO system will be able to continue to comply with particulate and opacity limits. If, however, an additional reduction in particulates and opacity become necessary, there are several engineering alternatives available, and they are also briefly discussed below.

Particulate and opacity calculations

This analysis is performed for a 150 MW utility boiler, burning 1.5% sulfur coal, having particulate emissions of 0.04 lb/mmBtu, post-ESP, or approximately 60 lb/hr, creating a stack plume opacity of 12-15%. In this case, the NOXSO adsorbers will generate 50 lb/hr of attrited sorbent. This is based on a total NOXSO plant attrition rate of 0.03% of the fluidized bed inventory per hour with 40% of this inventory being in the adsorbers.

The results of this analysis show particulate emissions decreasing while stack plume opacity increases. This occurs because the post-adsorber particle separators will remove the larger, more massive flyash and sorbent particles, but there will be an increase in the smaller sub-micron particles emitted, which have a greater effect on light scattering. Although there is an increase in the opacity, the analysis shows that the opacity will remain within the acceptable range of less than 20% visibility.

Particle size distributions

Both the particulate emissions and the stack plume opacity are dependent on the particle size distributions (PSD) of the flyash and the attrited sorbent. Based on NOXSO Proof-of-Concept (POC) test data from April 1993 in which the average particle size distributions were measured at the POC adsorber inlet and outlet and at the sorbent heater outlet, these PSDs are assumed to be as shown in Table 3-1. The POC adsorber inlet particulates are assumed to be representative of typical flyash PSD, measured post-ESP; while the fluidized bed sorbent heater's outlet particulates are taken to represent the PSD of attrited NOXSO sorbent. POC post-adsorber data is assumed to be unrepresentative of attrited sorbent because data only exists from sampling points downstream of the POC cyclone.

Table 3-1. POC Particle Size Distributions		
	Percent Weight Under Size	
Particle Diameter (microns)	Flyash exiting ESP	Attrited Sorbent
0.7	13.3	4.9
0.9	17.8	5.9
1.3	24.7	8.7
2.6	33.1	13.6
4.0	43.6	61.5
5.8	52.9	75.4
8.5	64.0	92.7
13.6	78.0	94.8

Particulate emissions

The points of control for particulate emissions in a NOXSO plant are the Breslove separators which will be immediately downstream of the adsorber vessels. Any particles, both flyash and attrited sorbent, which are not captured by this separator are transmitted to the plant stack. By summing the flyash and attrited sorbent particulates (110 lb/hr) and dividing by the assumed thermal input, the Breslove separators on the NOXSO adsorbers will see 0.07 lb/mmBtu of combined particulates. By applying the above particle size distributions to Breslove's published removal efficiency curves, it is calculated that the separator particulate removal efficiency will be 63% and that emissions from the separator will be 41 lb/hr or 0.027 lb/mmBtu, resulting in a net decrease over the plant's initial emissions of 0.04 lb/mmBtu. The results of this analysis, including the theoretical removal efficiencies for the separators, are presented in Table 3-2. To verify the published Breslove data on removal efficiency, laboratory testing will be conducted as explained in a later section of this report.

Table 3-2. Particulate Emissions					
PSD um	Mass in, lb/hr		Removal efficiency %	Mass out, lb/hr	
	Flyash	Sorbent		Flyash	Sorbent
>13.6	13.2	2.60	96	0.53	0.11
8.5-13.6	8.40	1.05	93	0.59	0.07
5.8-8.5	6.66	8.65	85	1.00	1.30
4.0-5.8	5.58	6.95	76	1.34	1.67
2.6-4.0	6.30	23.95	63	2.33	8.86
1.3-2.6	5.04	2.45	45	2.77	1.35
0.9-1.3	4.14	1.40	0	4.14	1.40
0.7-0.9	2.70	0.50	0	2.70	0.50
<0.7	7.98	2.45	0	7.98	2.45
Totals	60.0	50.0		23.38	17.71
	110.0		62.6	41.09	

Stack plume opacity

Opacity calculations are based on theory presented in "Calculation of Smoke Plume Opacity from Particulate Air Pollutant Properties" by D. S. Ensor and M. J. Pilat, which appeared in the August 1971 edition of the Journal of the Air Pollution Control Association. Theoretical calculations of opacity are based on the Bouguer law (Lambert-Beer law) which gives the attenuation of a collimated beam of light through a turbid medium over a given path length, as follows:

$$I/I_0 = \exp(-bL)$$

where I/I_0 is the fraction of transmitted light, L is the path length (m), and b is the light extinction coefficient of a volume of aerosol (m^{-1}).

Opacity is related to this equation by:

$$Op = 1 - I/I_0$$

The authors derive a relationship for the extinction coefficient, b, and produce an equation of the form:

$$I/I_0=\exp(-W*L/\rho/K)$$

where W is the particulate mass concentration (g/m^3), ρ is the average particle density (g/cm^3), and K is the specific particulate volume extinction coefficient ratio (cm^3/m^2). K is a function of the particle size distribution, particle refractive index, and the wavelength of light. The authors produce values of K for various refractive indices and for a wavelength of light of 550 nm, which is approximately the wavelength of maximum sensitivity for the human eye. Graphs of K versus geometric mass mean radius and geometric standard deviation are provided for typical black and white aerosols; it is these graphs which provide values of K for these calculations.

Assumptions made for the opacity calculations are as follows: the flue gas flow rate is 500,000 acfm, the stack diameter is 5m (or about 16 ft), and the density of the flyash is 2.0 g/cm^3. The density of attrited sorbent is taken to be 1.83 g/cm^3, which is the skeletal bulk density of the sorbent. Based on the results in Table 3-2, the particle size distributions of the flyash and the sorbent following the separator are assumed to be as shown in Table 3-3. Statistical analysis of the PSDs provides the respective geometric mass mean radii and geometric standard deviations, which are then used to obtain values of K.

Table 3-3. Post-separator PSDs

	Percent Weight Under Size		
Diameter,um	Flyash	Sorbent	Combined
0.7	34.13	13.83	25.38
0.9	45.68	16.65	33.16
1.3	63.39	24.56	46.64
2.6	75.24	32.18	56.67
4.0	85.2	82.21	83.90
5.8	90.93	91.64	91.23
8.5	95.21	98.98	96.83
13.6	97.73	99.38	98.44

Opacity results

The results of the opacity analysis are presented in Figure 3-2 through Figure 3-5. Figure 3-2 shows that the opacity before installation of a NOXSO system is 14.8%, while Figure 3-3 shows that the opacity of the integrated NOXSO system is 17.3%. To account for this increase in opacity, Figure 3-4 shows that the flyash contribution to the post-NOXSO opacity is 11.7%, or a decrease of about 3%, while Figure 3-5 shows that the sorbent contribution to the opacity is about 5%, resulting in a net increase of 2-3%. Although there is a slight increase in the opacity, it remains within the compliance requirement of less than 20%. The combined opacity of Figures 3-4 and 3-5 is nearly equal to the opacity calculated in Figure 3-3, as expected. This is expected because opacity is considered to be additive, that is, the light scattering of one particle is independent of the light scattering of any other particles.

Several assumptions are required to make this analysis possible. First, the analysis assumes that the particle size distributions are log-normal distributions, in order to evaluate the geometric mass mean radius and geometric standard deviation. Also, the PSDs are assumed to be constant, although it is much more likely that the PSDs and the particulate concentrations vary over wide ranges. Additionally, a fundamental part of the analysis is the use of Mie electromagnetic scattering theory for spherical particles. While Mie theory has been applied to single spherical particles and clouds of spherical particles, the light extinction of irregularly shaped particles, in random motion, with sizes near the wavelength of light is not completely understood.

Engineering alternatives are reviewed and evaluated for possible implementation, should it become necessary to decrease either the particulate emissions or plume opacity.

Available options for further reductions

If either engineering evaluations or actual experience indicate that increased performance is required, particulate emissions and opacity may be reduced by several methods. The simplest and most direct means is to install standard Breslove suction devices to the solids discharge point of the installed separators. This change has a modest cost and would increase NOXSO system electrical requirements only slightly. Another option may be to install a barrier filter device for a portion of the gas volume, sufficiently sized to ensure particulate and opacity compliance. There are several other options available for implementation if the need should arise. Although further analysis and testing are required, NOXSO is confident that proper engineering of the NOXSO system will allow any boiler to maintain compliance with state and local regulations.

3.3.3 Separator Performance Test

The demonstration plant design employs centrifugal separators at the flue gas outlet of the adsorbers. The primary purpose of the separators is to remove the attrited sorbent from the gas stream. The attrited sorbent is then sent to the boiler via the NO_x recycle stream where it mixes and is removed with the boiler ash products. If the efficiency of the separators is high enough, they will remove a portion of the flyash in the flue gas not removed by the ESP producing a net reduction in particulate emissions with the addition of the NOXSO plant.

Figure 3-2. Calculation of Opacity for Pre-NOXSO Flyash Emissions

ASSUMPTIONS:

1.) 60 lb/hr OF PARTICULATES AT 500,000 ACFM.
2.) PARTICLE SIZE DISTRIBUTION ACCORDING TO POC ADSORBER INLET.
3.) AVERAGE PARTICLE DENSITY OF 2.0 g/cc.
4.) STACK EXIT DIAMETER OF 5 m OR 16.4 ft.

SIZE RANGE D,um	MIDRANGE SIZE Di, um	% MASS IN RANGE %	% MASS LESS THA INDICATED	MASS IN RANGE lb/hr	MASS IN RANGE g/hr
>13.6	20	22.00	100	13.20	5987.52
8.5-13.6	11.05	14.00	78	8.40	3810.24
5.8-8.5	7.15	11.10	64	6.66	3020.98
4.0-5.8	4.9	9.30	52.9	5.58	2531.09
2.6-4.0	3.3	10.50	43.6	6.30	2857.68
1.3-2.6	1.95	8.40	33.1	5.04	2286.14
0.9-1.3	1.1	6.90	24.7	4.14	1877.90
0.7-0.9	0.8	4.50	17.8	2.70	1224.72
<0.7	0.35	13.30	13.3	7.98	3619.73
		100		60.00	27216.00

GEOMETRIC MASS MEAN DIAMETER, Dg =	4.055 um
GEOMETRIC STANDARD DEVIATION, GSD =	3.885
FROM BLACK AEROSOL GRAPH, K =	0.5 cm^3/m^2
PARTICLE CONCENTRATION, W =	0.032 g/m^3
OPACITY = 1-EXP(-W*L/(K*RHO)) =	14.80 %

Figure 3-3. Calculation of Opacity for Combined Flyash and Sorbent Emitted after the Breslove Separator

ASSUMPTIONS:

1.) 41.09 lb/hr OF PARTICULATES AT 500,000 ACFM.
2.) PSD ACCORDING TO POC RESULTS AND BRESLOVE SEPARATOR EFFICIENCY FOR FLYASH AND SORBENT COMBINED.
3.) AVERAGE PARTICLE DENSITY BASED ON PARTICULATE COMPOSITION OF 57% FLYASH AND 43% SORBENT, OR 1.926 g/cc.
4.) STACK EXIT DIAMETER OF 5 m OR 16.4 ft.

SIZE RANGE D,um	MIDRANGE SIZE Di, um	% MASS IN RANGE %	% MASS LESS THA INDICATED	MASS IN RANGE lb/hr	MASS IN RANGE g/hr
>13.6	20	1.56	100	0.64	290.30
8.5-13.6	11.05	1.61	98.33	0.66	299.38
5.8-8.5	7.15	5.60	96.56	2.30	1043.28
4.0-5.8	4.9	7.33	91.2	3.01	1365.34
2.6-4.0	3.3	27.23	84.17	11.19	5075.78
1.3-2.6	1.95	10.03	60.06	4.12	1868.83
0.9-1.3	1.1	13.48	49.69	5.54	2512.94
0.7-0.9	0.8	7.78	35.44	3.20	1451.52
<0.7	0.35	25.38	26.97	10.43	4731.05
		100		41.09	18638.42

GEOMETRIC MASS MEAN DIAMETER, Dg = 1.542 um
GEOMETRIC STANDARD DEVIATION, GSD = 2.959
FROM WHITE & BLACK AEROSOL GRAPHS, K = 0.3 cm^3/m^2
PARTICLE CONCENTRATION, W = 0.022 g/m^3

OPACITY = 1-EXP(-W*L/(K*RHO)) = 17.29 %

Figure 3-4. Calculation of Opacity for Flyash Emitted after the Breslove Separator

ASSUMPTIONS:

1.) 23.38 lb/hr OF PARTICULATES AT 500,000 ACFM.
2.) PARTICLE SIZE DISTRIBUTION ACCORDING TO POC ADSORBER INLET AND BRESLOVE SEPARATOR EFFICIENCY.
3.) AVERAGE PARTICLE DENSITY OF 2.0 g/cc.
4.) STACK EXIT DIAMETER OF 5 m OR 16.4 ft.

SIZE RANGE D,um	MIDRANGE SIZE Di, um	% MASS IN RANGE %	% MASS LESS THA INDICATED	MASS IN RANGE lb/hr	MASS IN RANGE g/hr
>13.6	20	2.27	100	0.53	240.41
8.5-13.6	11.05	2.52	97.74	0.59	267.62
5.8-8.5	7.15	4.28	95.23	1.00	453.60
4.0-5.8	4.9	5.73	90.95	1.34	607.82
2.6-4.0	3.3	9.96	85.22	2.33	1056.89
1.3-2.6	1.95	11.85	75.25	2.77	1256.47
0.9-1.3	1.1	17.71	63.36	4.14	1877.90
0.7-0.9	0.8	11.55	45.68	2.70	1224.72
<0.7	0.35	34.13	34.13	7.98	3619.73
		100		23.38	10605.17

GEOMETRIC MASS MEAN DIAMETER, Dg =	1.144 um
GEOMETRIC STANDARD DEVIATION, GSD =	3.034
FROM BLACK AEROSOL GRAPH, K =	0.25 cm^3/m^2
PARTICLE CONCENTRATION, W =	0.012 g/m^3
OPACITY = 1-EXP(-W*L/(K*RHO)) =	11.74 %

Figure 3-5. Calculation of Opacity for Sorbent Emitted after the Breslove Separator

ASSUMPTIONS:

1.) 17.71 lb/hr OF PARTICULATES AT 500,000 ACFM.
2.) PARTICLE SIZE DISTRIBUTION ACCORDING TO POC SORBENT HEATER OUTLET AND BRESLOVE SEPARATOR EFFICIENCY.
3.) AVERAGE PARTICLE DENSITY OF 1.827 g/cc.
4.) STACK EXIT DIAMETER OF 5 m OR 16.4 ft.

SIZE RANGE D,um	MIDRANGE SIZE Di, um	% MASS IN RANGE %	% MASS LESS THA INDICATED	MASS IN RANGE lb/hr	MASS IN RANGE g/hr
>13.6	20	0.62	100	0.11	49.90
8.5-13.6	11.05	0.40	99.4	0.07	31.75
5.8-8.5	7.15	7.34	98.99	1.30	589.68
4.0-5.8	4.9	9.43	91.65	1.67	757.51
2.6-4.0	3.3	50.03	82.24	8.86	4018.90
1.3-2.6	1.95	7.62	32.19	1.35	612.36
0.9-1.3	1.1	7.91	24.57	1.40	635.04
0.7-0.9	0.8	2.82	16.66	0.50	226.80
<0.7	0.35	13.83	13.84	2.45	1111.32
		100		17.71	8033.26

GEOMETRIC MASS MEAN DIAMETER, Dg =	2.286 um
GEOMETRIC STANDARD DEVIATION, GSD =	2.483
FROM WHITE AEROSOL GRAPH, K =	0.5 cm^3/m^2
PARTICLE CONCENTRATION, W =	0.009 g/m^3

OPACITY = 1-EXP(-W*L/(K*RHO)) =	5.04 %
TOTAL = SORBENT OPACITY PLUS FLYASH OPACITY	16.78 %

The centrifugal separator selected is a straight through flow type. The manufacturer of this separator claims high separation efficiency with a very low pressure drop. Using performance data from the manufacturer and particulate size distribution and loading data from the POC, a separation efficiency of greater than 60% is estimated. This is high enough to produce a net reduction in particulate emissions. To determine the actual efficiency, a test will be performed.

The manufacturer of the separator has supplied a single module, many modules would make up a demonstration plant separator. This module is eight feet long and twenty-seven inches in diameter, a size and capacity which can be tested in the NOXSO lab. Two sections of straight ductwork have been fabricated and will be located upstream and downstream of the separator module. The duct sections have a length equivalent to 10 diameters in accordance with EPA method 2. This equipment is being assembled in the NOXSO lab for the purpose of conducting the tests.

The dust that will be used for the tests was collected from the POC baghouse. It consists of attrited sorbent fines and flyash which is representative of the particulates that will be entering the demonstration plant separators. The dust will be fed into the gas stream at a rate producing a loading of about 0.07 grains/cubic foot. This particulate loading was determined from a typical PC fired boiler with a 99.1 % ESP efficiency and the latest sorbent attrition data. Higher and lower loading and gas velocities will also be tested.

A known amount of dust will be introduced into the gas stream over a test period. At the end of the test period, the separator dust hopper will be emptied. The overall separator efficiency will be determined by comparing the mass of the dust that entered the separator to that removed from the hopper. A particle size distribution will be performed on a sample of the dust entering the separator and on a sample removed from the dust hopper. This data will allow the construction of a grade efficiency curve. In-duct dust sampling will be performed using the guidance of EPA method 5. Gas velocity and flow will be determined in accordance with EPA method 2.

3.4 Nitrogen Oxide Studies

No nitrogen oxide studies were conducted during this reporting period.

3.5 Process Studies

3.5.1 POC Equipment Inspection and Material Evaluation

The POC facility in Toronto, Ohio, was examined and material samples were removed prior to the start of demolition. The examination was performed to determine how materials used in construction of the POC withstood operation. The work performed included 1) ultrasonic measurements of metal thickness, 2) marking and collection of equipment samples, 3) visual examination of equipment, and 4) recovery of the corrosion coupon rack in the bottom head of the sorbent heater.

The vessels and ductwork of the POC were examined using ultrasonic testing on April 8, 1994. Metal thickness measurements were performed on the adsorber, sorbent heater, sorbent cooler, adsorber cyclone, regenerator, and adsorber inlet ductwork. The only significant metal loss occurred on the adsorber inlet ductwork. All the other ultrasonic test measurements of metal thickness showed no significant metal loss.

Figure 3-6 shows the measured duct metal thickness as a function of distance and position along the ductwork. This duct was originally coated internally with a corrosion resistant coating. None of this coating remained in the duct and it probably disappeared early in the operation of the POC. The ductwork in the water spray area developed a hole and required repair near the end of the project. At this time, we discovered a corrosion related malfunction in the spray nozzle head for the water spray. This caused the water spray to impinge directly on the duct, cooling the metal, and causing acid condensation on the duct. The ultrasonic thickness measurements show that the most severe corrosion was limited to the 20 feet of ductwork directly downstream of the water spray. The remaining ductwork showed only slightly smaller metal thickness than the duct before the water spray. The original duct thickness was specified as 0.187 inches minimum. Conclusions from the duct examination are 1) the original internal coating of the ductwork did not survive the environment. Reports of such duct coatings in the literature also show that all coatings fail in relatively short periods in this type of environment, and 2) the in-duct spraying of water into flue gas ductwork is especially corrosive. It should be noted that this method of flue gas cooling will not be employed at the demonstration plant due to the corrosion problem which it creates.

The demolition of the POC presents a unique opportunity to collect and examine samples of the process equipment. This will reveal exactly how well (or how poorly) materials used in the POC withstood the operations. These samples (and their analysis) will complement the results from corrosion coupons placed in the POC equipment. Table 3-4 is a list of the POC samples and planned analysis. The samples were each marked and photographed on the process prior to removal. Samples were collected by either unbolting the sample from the apparatus or by cutting samples from the equipment with an oxygen-acetylene torch. These samples are considered archive samples by NOXSO and will be kept and stored after analysis. This will allow additional tests of POC samples to be performed in the future if desired.

Figure 3-6. Adsorber Duct Thickness

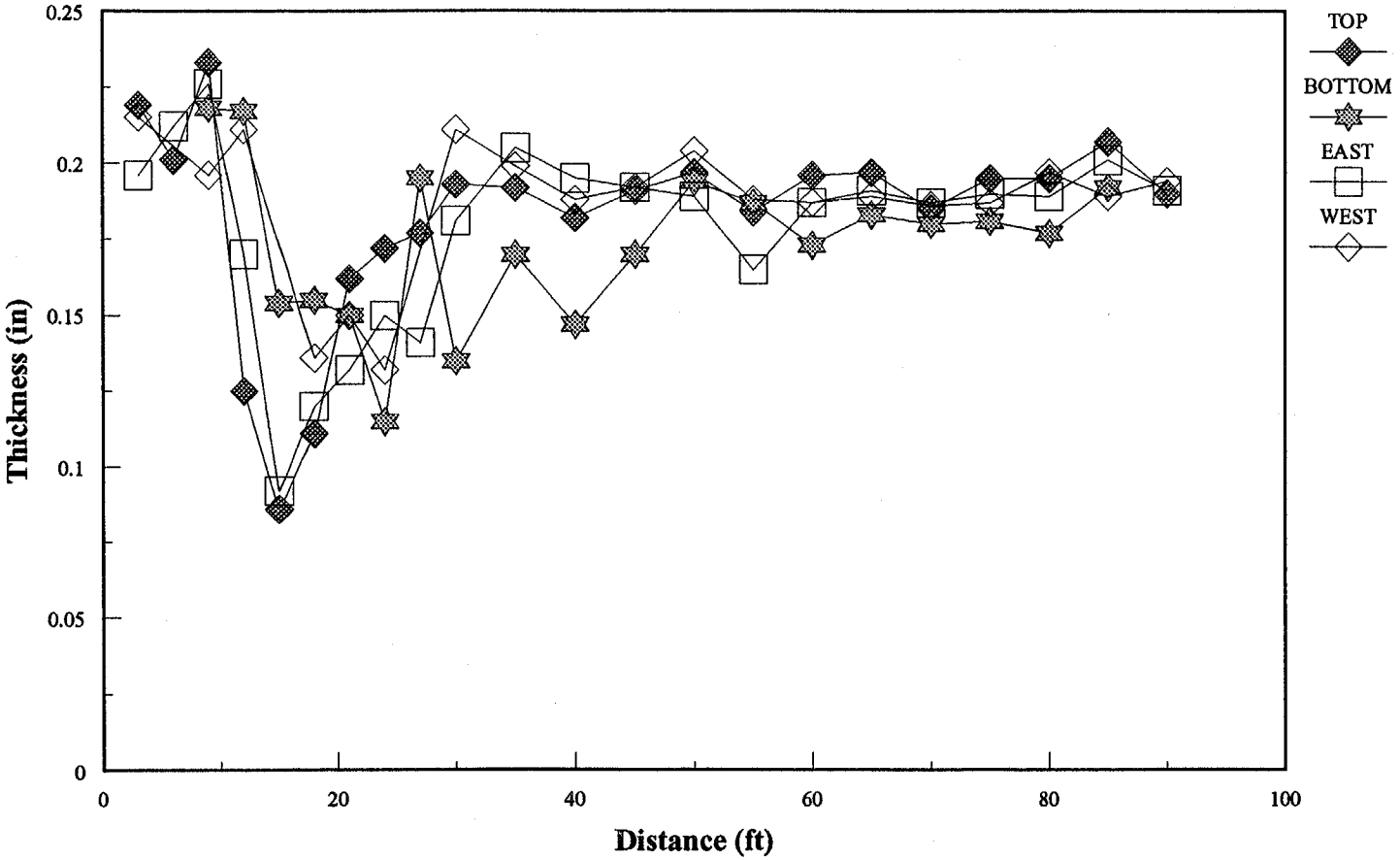

Table 3-4. Summary of POC Demolition Samples, for Analysis of Corrosion and Erosion

	Corrosion Sample	Size	Analysis
1	Adsorber section (bottom bed)	6"X3'	thickness
2	Adsorber shell section (near top side of adsorber)	12"X12"	thickness
3	Adsorber grid (upper bed)	12"x12"	thickness, hole size
4	Adsorber grid (bottom bed)	12"x12"	thickness, hole size
5	Adsorber grid support (from center of vessel)	4"x12"	thickness, coating condition
6	Flue gas inlet ductwork (side of duct just before elbow at base of adsorber)	12"x12"	thickness, coating condition, pitting
7	Flue gas outlet ductwork (side of duct, straight section)	12"x12"	thickness
8	Regenerator wall section (upper regenerator, with welds between plates and top head)	12"x12"	cut & polish, alon thickness and weld corrosion
9	Regenerator wall section (middle regenerator, with welds between plates and in sorbent section)	12"x12"	cut & polish, alon thickness and weld corrosion
10	Regenerator wall section (middle regeneration, section with visible pitting of weld heat affected zones)	12"x12"	cut & polish, alon thickness and weld corrosion
11	Steam treater wall section (upper steam treater, with welds between plates)	12"x12"	omitted this sample
12	Steam treater wall section (lower steam treater in sorbent section, with welds between plates)	12"x12"	cut & polish, alon thickness and weld corrosion
13	Air heater expansion joint (also visual examination of entire unit)	12"x24" entire joint	thickness and analysis of joint failure
14	Upper J-valve downcomer section	6"x6" diameter	cut & polish, alon thickness, chloride analysis
15	Middle J-valve downcomer section	6"x6" diameter	cut & polish, alon thickness, chloride analysis

Table 3-4. Summary of POC Demolition Samples, for Analysis of Corrosion and Erosion

	Corrosion Sample	Size	Analysis
16	Sorbent heater section (bottom bed section)	6"x3'	thickness
17	Sorbent heater bottom head section	12"x12"	thickness
18	Sorbent cooler section (top bed section)	6"x3'	thickness
19	Sorbent heater grid (bottom bed)	12"x12"	thickness, hole diameter
16	Regenerator thermowell (446 thermowell, top of thermowell)	12"x1.5" diameter	thickness, corrosion
17	Regenerator thermowell (446 thermowell, top middle section)	12"x1.5" diameter	thickness, corrosion
18	Regenerator thermowell (446 thermowell, bottom middle section)	12"x1.5" diameter	thickness, corrosion
19	Regenerator thermowell (446 thermowell, bottom section)	12"x1.5" diameter	thickness, corrosion
20	Regenerator off-gas piping	12"x3" diameter	cut & polish, alon thickness
21	Steam treater off-gas piping	12"x3" diameter	cut & polish, alon thickness
22	Dense phase lift lower elbow		cut, thickness
23	Dense phase lift upper elbow		cut, thickness
24	Ductwork between air heater and sorbent heater	12"x12"	thickness
25	Combined steam treater and regenerator off-gas piping (near incinerator)	12" long	cut & polish, alon thickness
26	Top J-valve expansion joint		initial visual inspection
27	Mid J-valve expansion joint		initial visual inspection

Table 3-4. Summary of POC Demolition Samples, for Analysis of Corrosion and Erosion			
	Corrosion Sample	Size	Analysis
28	Corrosion coupon rack, sorbent heater inlet		visual, weights and thickness of each coupon
29	Middle grid support for sorbent heater (at repair of weld crack)	12"x4"	chloride cracking
30	Top J-valve elbow		cut & polish, alon and metal thickness
31	Top L-valve box		
32	Middle J-valve box		
33	Middle J-valve elbow		cut & polish, alon and metal thickness
34	Adsorber inlet water spray nozzles (2)		visual
35	Dense phase conveyor inlet butterfly valve		visual
36	Regenerator outlet gas control valve (PV-518)		visual, cut and examine
37	Regenerator off-gas outlet elbow		
38	Steam treater off-gas control valve (PV-308)		visual
39	Regenerator off-gas thermowell (TE-316)		thickness, corrosion and pitting
40	Regenerator off-gas valve (CV-3022)		visual
41	Top J-valve thermowell		visual, thickness and erosion rate
42	Regenerator pressure safety valve (PSV-3030)		visual, determine cause of failure if possible
43	Steam treater bottom cone section (at steam inlet)	12"x24" cone section	visual, possible cut+polish, alon thickness, chlorides
44	Hastalloy spray nozzle (removed from adsorber inlet ductwork)		visual, determine incorrect metal on spray nozzle
45	Regenerator sorbent sample port	1"x3'	visual, cut & polish, alon thickness and condition
46	Section of sorbent heater grid with crack at wall	12"x12"	visual, chlorides

A visual examination of the POC equipment was performed to determine material and equipment suitability. Observations from this examination are as follows:

The regenerator was in excellent condition, with no signs or indications of cracking or corrosion through the inside alon surface. The one exception to this was some pitting of each side of a weld where the regenerator support was located. This did not become larger during the project, and it has been taken as a sample for further analysis.

Approximately 20-25% of the Martex coating in the bottom shell of the adsorber had flaked off exposing the underlying metal (carbon steel). Corrosion of the exposed metal was minimal.

The flue gas inlet thermowell (TE-107) was missing about 1/2 of its teflon coating. The missing coating was on the upstream side of the thermowell, indicating that the loss was caused primarily by erosion of the coating. Teflon coated thermowells should not be used on future installations.

All of the vessels were in excellent condition, with no visible wear or metal loss.

The ductwork at the adsorber fan entrance was corroded at the inlet pressure tap. This tap had been used as the liquid SO_2 injection point and had already been patched once during the project. The rapid corrosion in this area was due to the cooling of the carbon steel by vaporizing SO_2. The cool metal condensed acid from the flue gas resulting in rapid corrosion of the metal. Future SO_2 injection systems must be more carefully designed to avoid the formation of cold spots with rapid corrosion.

The expansion pipe between the air heater and the sorbent heater developed cracks on the inside edges of the bellows. This will be examined to find the cause of failure but was most likely caused by overheating of the expansion joint. This was not equipped with a internal liner which would have probably prevented this problem.

All of the alonized surfaces in the off-gas ductwork looked excellent. No corrosion or attack on the alon surface was visible. In contrast, substantial corrosion was found on the regenerator pressure control valve (PV-518). This valve had a body of 316 SS. An unalonized thermowell in the off-gas line (TE-316) also showed substantial corrosion.

The spiral wound gaskets used in the assembly of the POC looked excellent. There was some minor attack on the gaskets used in the regenerator off-gas lines and the sorbent conveying lines. This attack was confined to the innermost part of the gasket (where the gasket contacted the gas).

The regenerator pressure relief valve (PSV-3030) was found to be partly open and its outlet was 1/2 full of elemental sulfur. The most likely cause of this is the PSV opened, and then did not close fully when the system pressure returned to normal. (Either sorbent or sulfur may have prevented closure. This valve will be disassembled and

examined to determine the cause of its failure.) Future PSV's connected to the regenerator should be modified to allow integrity checks.

The corrosion coupon rack in the bottom head of the sorbent heater was recovered for analysis. This coupon rack was placed into the vessel at the start of the project and was exposed to 10,834 hours of air heater operation (446 on/off cycles of the air heater). This rack could not be removed earlier in the project because it was below the bottom grid of the sorbent heater and could not be accessed without cutting the sorbent heater grid. The carbon steel mounts of this coupon rack had spilled and the rack had fallen into the bottom head of the sorbent heater. It was covered in sorbent which had fallen into the bottom head of the vessel. The coupons on the rack are currently being examined.

3.5.2 Adsorber/Regenerator Computer Model

Simulation of the POC Fluid-bed Sorption Data

In the last quarter, we developed a computer program to simulate the fluid-bed adsorber. As mentioned in the last quarterly report, the program used one adjustable parameter to apply the 2-inch fixed-bed test results to predict the 126 inch POC fluid-bed tests. The program simulated the SO_2 and NO_x removal efficiencies well, but predicted the off-gas NO_2 concentration poorly. Therefore, an empirical off-gas-NO/NO_2 relationship was developed as an alternative for the adsorber design. To improve the adsorber model, we need more laboratory test data, especially in the NO and NO_2 sorption study. While the laboratory was busy in other test activities, we were working on a computer program which simulates the multi-stage fluid-bed adsorber.

The program for simulating a multi-stage fluid-bed adsorber was developed. However, the program runs slowly and has convergence difficulties. For each stage, the program solves nested nonlinear equation sets to obtain the mean gas concentrations for integrating the solid phase reactions and vice versa. The convergence of the material balance is heavily dependent upon the initial guessed values. Currently, we are searching for a better way to speed up the program.

Regenerator Model

Based on the regeneration test studies, the following reaction scheme was proposed to explain the regeneration of the spent sorbent with either H_2S, H_2, CO, or CH_4.

1. $H_2S + Na_2SO_4 + Al_2O_3 \rightarrow 2\ NaAlO_2 + SO_2 + H_2O + 1/x\ S_x$
2. $2\ H_2S + SO_2 \rightarrow 2\ H_2O + 3/x\ S_x$
3. $H_2 + Na_2SO_4 + Al_2O_3 \rightarrow 2\ NaAlO_2 + SO_2 + H_2O$
4. $3\ H_2 + SO_2 \rightarrow H_2S + 2\ H_2O$
5. $H_2 + 1/x\ S_x \rightarrow H_2S$
6. $CO + Na_2SO_4 + Al_2O_3 \rightarrow 2\ NaAlO_2 + SO_2 + CO_2$
7. $3\ CO + SO_2 \rightarrow COS + 2\ CO_2$

8. $CO + H_2O \rightarrow CO_2 + H_2$
9. $CO + 1/x\ Sx \rightarrow COS$
10. $COS + H_2O \rightarrow H_2S + CO_2$
11. $CH_4 + 4\ Na_2SO_4 + 4\ Al_2O_3 \rightarrow 8\ NaAlO_2 + 4\ SO_2 + CO_2 + 2\ H_2O$
12. $CH_4 + SO_2 \rightarrow CO_2 + H_2 + H_2S$
13. $CH_4 + H_2O \rightarrow CO + 3\ H_2$
14. $CH_4 \rightarrow C + 2\ H_2$
15. $C + 2/x\ S_x \rightarrow CS_2$
16. $CS_2 + 2\ H_2O \rightarrow CO_2 + 2\ H_2S$
17. $C + H_2O \rightarrow CO + H_2$

The modeling method is similar to Dr. Froment's molecular reaction scheme approach which he used to model the dehydrogenation of propane, butane, butence and butadience ("Modeling of Thermal Cracking Kinetics," Chemical Engineering Science, Vol.302, P.601-617,1976). The reactions for the CH_4 dissociation to form free radicals, CH_3 and H, and subsequently polymerizations to form C_2H_6 etc. were excluded. Reactions 1 and 2 are those for using H_2S as the only reducing gas. Reactions 1 though 5 are for using H_2 to regenerate the spent sorbent. Reactions 6 and 7 are for CO only regeneration. Reactions 1 through 10 are for using reforming gas as regenerant. Reactions 1 through 17 are for CH_4 regeneration.

Obviously, the curve-fitting of the regeneration data to extract the rate constants are more difficult than that of adsorption. But, using a series of experiments, we can sequentially obtain all the rate constants. The concept is to conduct the regeneration test using only one reducing gas. For example, H_2S regeneration alone determines the rate constants of reactions 1 and 2. And H_2 regeneration determines the rate constants for reactions 3 through 5. CO regeneration gives rate constants for reactions 6 and 7. CO plus steam determines rate constants for reactions 8 to 10. The remaining seven rate constants are determined from the CH_4 regeneration data. These seven rate constants are obtained in two steps. First, the curve-fit task will concentrate on correlating the CH_4 off-gas concentration profile to extract the rate constants for reactions 11 through 13. Then the second correlation with the entire concentration profiles determines the rate constants for reactions 14 through 17. In this way, we use no more than four unknowns to fit one experimental result. Of course, each experiment has to be conducted isothermally.

Before collecting all the required experimental data in the laboratory, one computer simulation run was conducted with the CH_4 regeneration data. The test was conducted at 650°C in a 3/4-inch fixed-bed reactor, and used 4.68 l/hr CH_4 to treat 12.21 g SSA sorbent loaded with 3.08 wt% sulfur. The off-gas CH_4, SO_2 and H_2S concentration profiles were used to adjust the rate constants for reactions 11, 12 and 13. The rest of the rate constants were fixed at the assumed values. Figure 3-7 shows the simulation result, which resembles the off-gas concentration profiles.

To test the proposed reaction scheme further, we used the same rate constants to simulate the sorbent regeneration with different sulfur contents. All the regeneration experiments were conducted using the same conditions as the test with 3.08 wt% sulfur. The comparison between the simulated and measured data is shown in Figure 3-8, Figure 3-9, and Figure 3-10. These

Figure 3-7. CH4 Regeneration at 650 C

3.08 wt% S Sulfated Sorbent

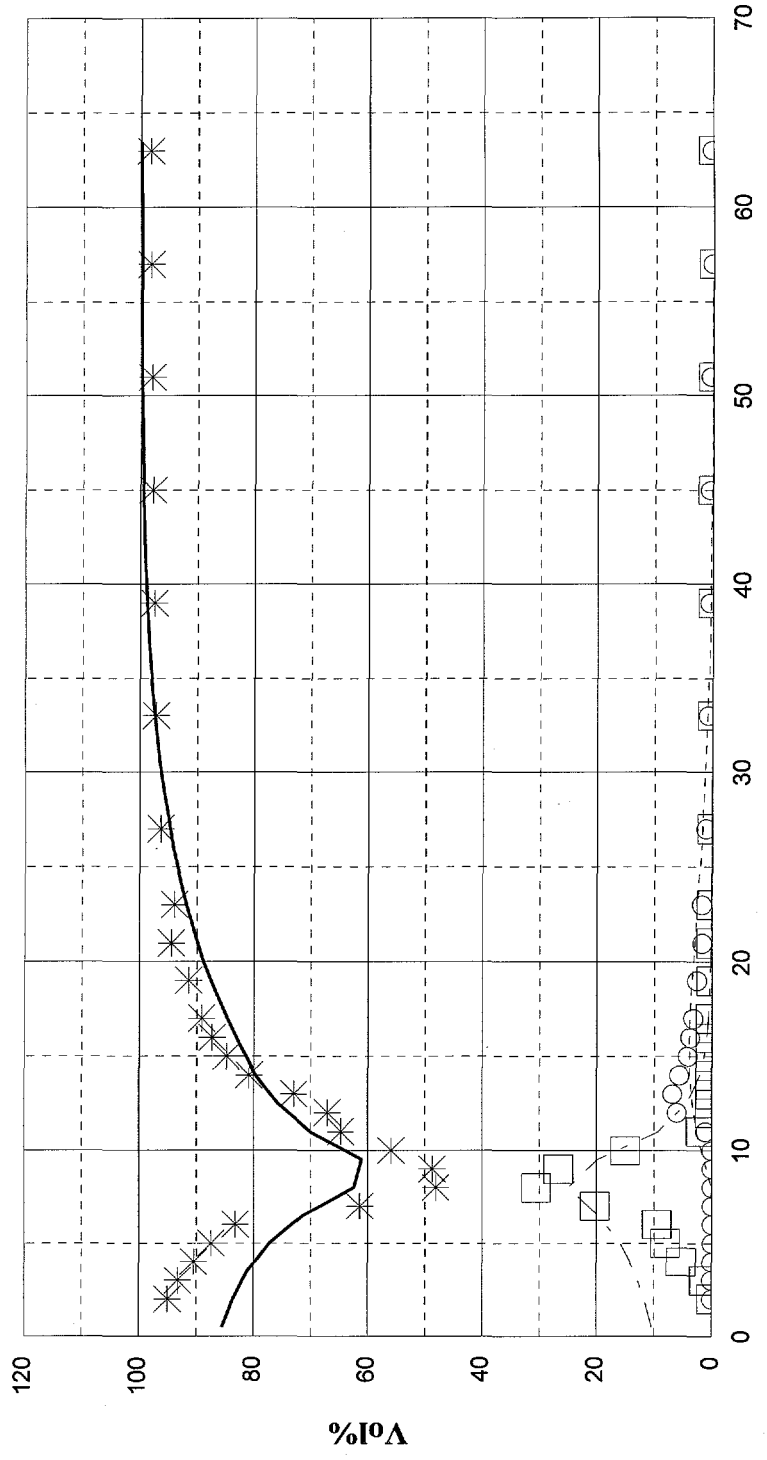

3.08 wt% sulfur

Figure 3-8. CH4 Regeneration at 650 C
2.53 wt% S Sulfated Sorbent

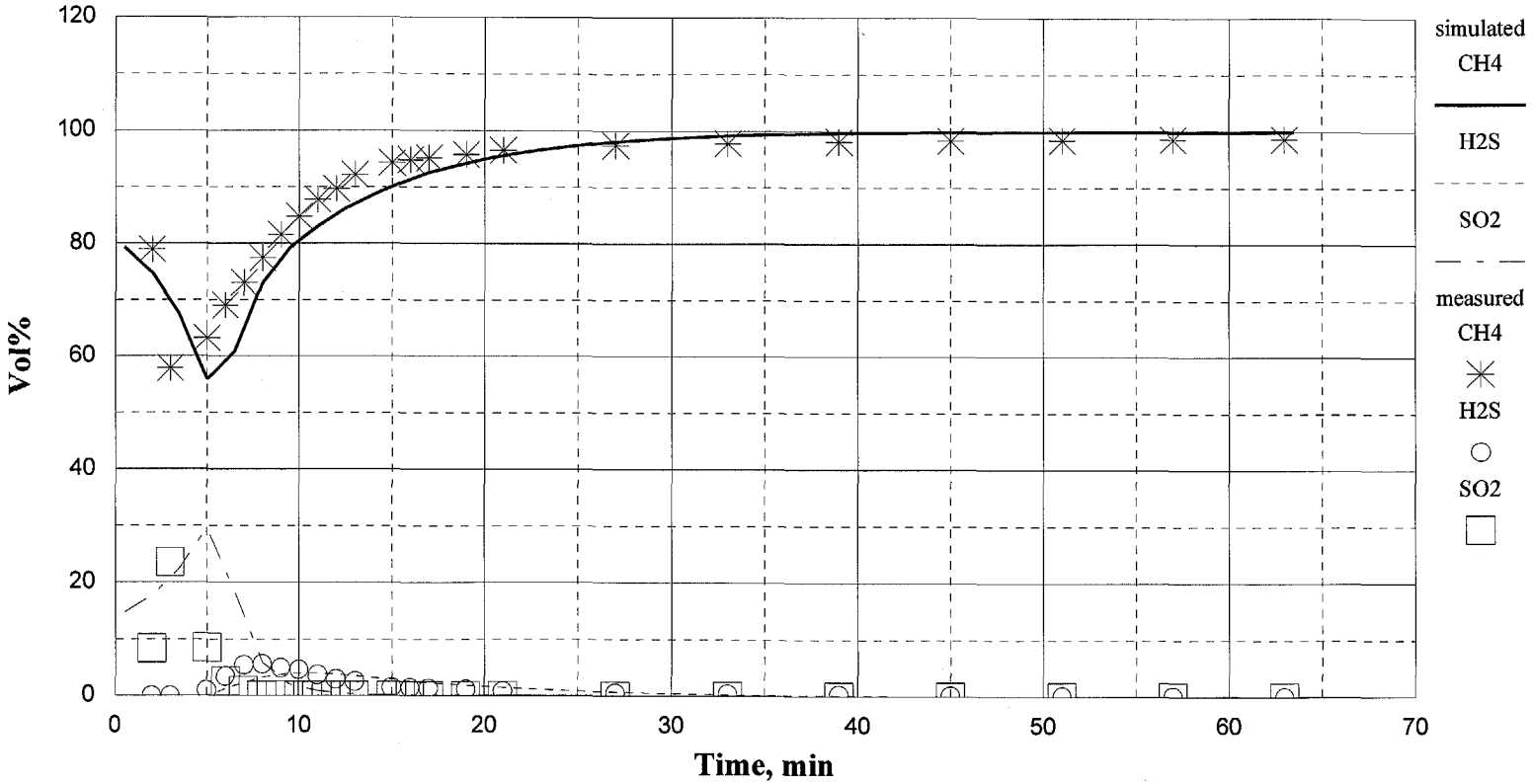

2.53 wt% sulfur

Figure 3-9. Sulfur CH4 Regeneration at 650 C
2.10 wt% S Sulfated Sorbent

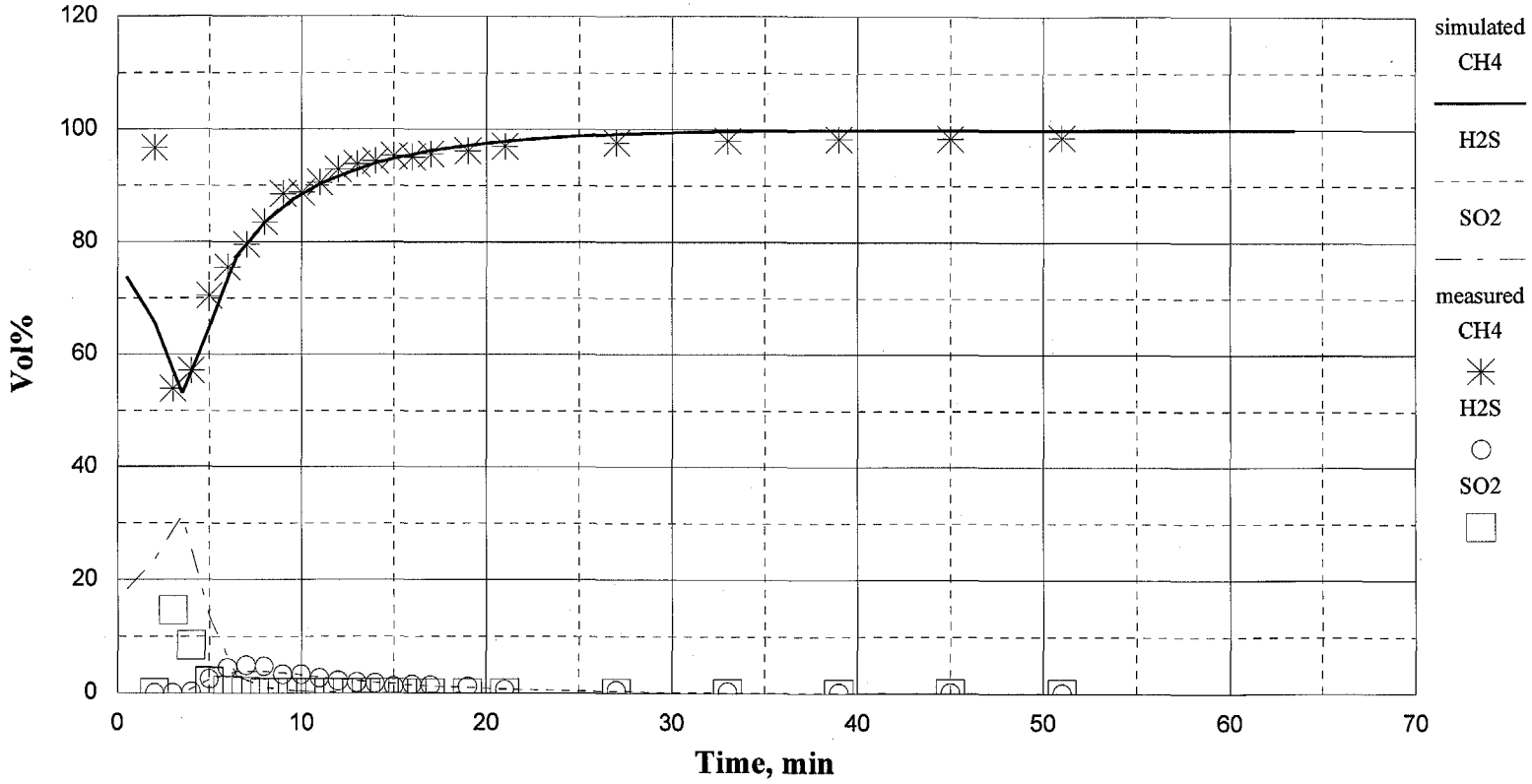

2.10 wt% sulfur

Figure 3-10. CH4 Regeneration at 650 C
1.55 wt% S Sulfated Sorbent

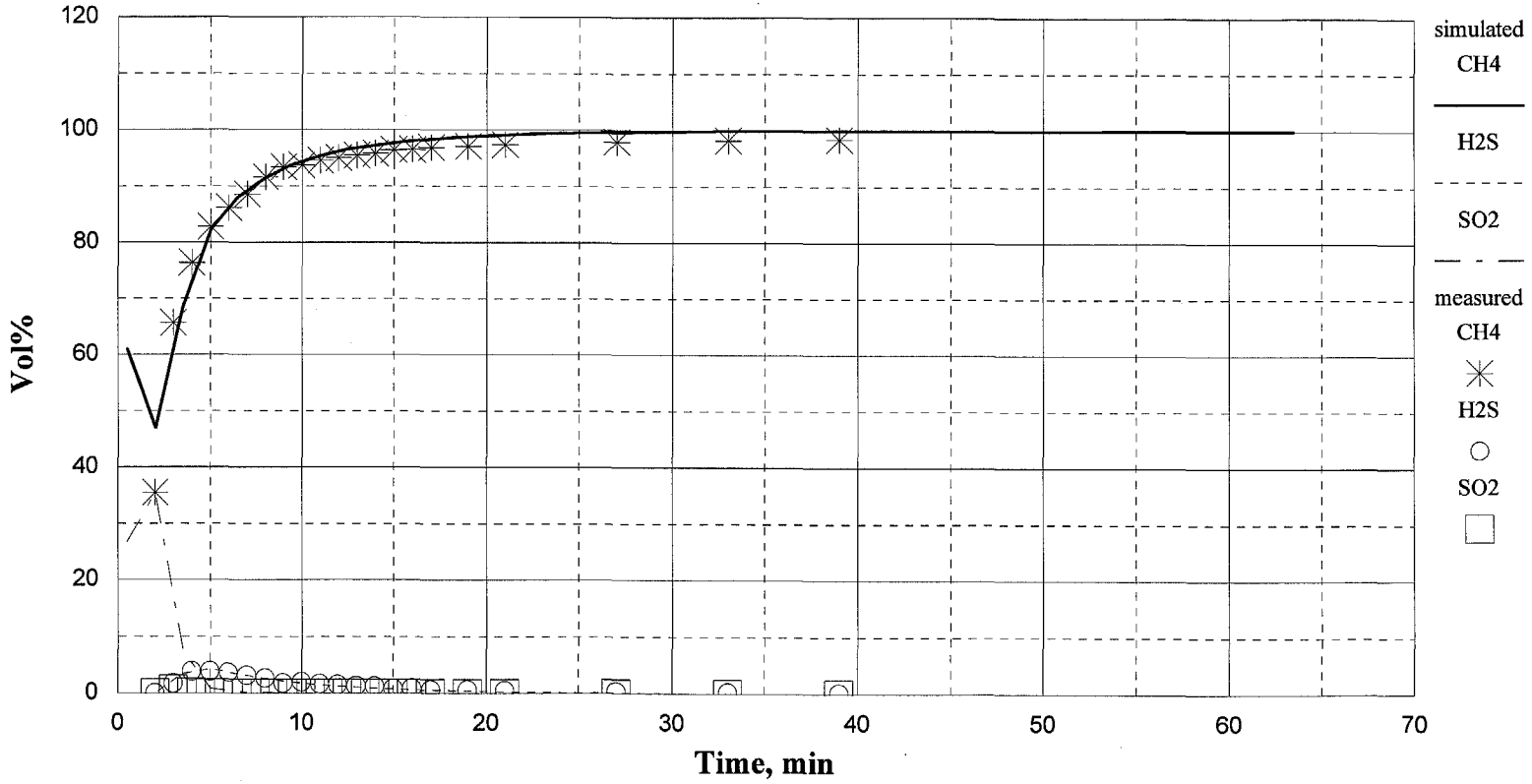

1.55 wt% sulfur

are for sorbent sulfur contents equal to 2.53, 2.10 and 1.55 wt%, respectively. Except for the initial times, the simulation results agree with the measured data well.

3.5.3 Process Simulation

To maintain the usefulness of the NOXSO process simulation program as a design tool, the program code is continuously updated and enhanced to reflect process refinements and to produce more rigorous results. During the last quarter, process refinements incorporated into the process simulator code included combining the separate methane and steam treater vessels into a single vessel and replacing the sorbent cooler to surge bin dense phase sorbent transport system with a dilute phase L-valve transport system. These and other process refinements incorporated into the process simulator are discussed in previous quarterly reports. In addition to process refinements, several process simulation subroutines were rewritten to produce more rigorous results. For example, the vessel heat loss routine was rewritten to include both radiant and natural convection heat losses.

During the last quarter, work was also begun to code an off design version of the process simulator. The NOXSO process simulation program is used to develop the material and energy balances and size the required rotating equipment and vessels for a NOXSO system operating at the base design conditions. The off design simulation program will model the base design NOXSO system operating at a set of conditions different than the base design conditions. For example, how will a NOXSO system designed to treat 300,000 scfm of flue gas operate when the flue gas flow rate from the power plant is reduced by 50% to 150,000 scfm. The off design simulation, using the base design equipment and vessel sizes, will calculate the material and energy balances for the new operating conditions. Also, the off design simulator can be used to determine the low cost operating conditions for these off design operating conditions by varying process parameters and noting their effect on the consumption of water, natural gas, power, and sorbent. The off design simulation program is currently being debugged and verified for accuracy.

3.5.4 Sorbent Water Adsorption Capacity

Previously, it was proposed that water adsorption and desorption in the NOXSO Process was the cause for the deficient energy balance closures experienced at the pilot plant. This proposal has been qualified through an examination of heat utilization efficiencies and by an uncertainty analysis (presented in Quarterly Technical Report No. 11). In order to quantify this effect, it is necessary to experimentally generate a set of water adsorption isotherms specific to the NOXSO sorbent. A complete set of adsorption isotherms would require an extensive laboratory effort. In order to obtain more immediate data, laboratory adsorption tests simulating water adsorption in the adsorber using NOXSO low density sorbent have been conducted. The result of this testing has been the resolution of the energy balance closures for both the heater and cooler. The adsorption characteristics of the NOXSO sorbent generated in the lab compare favorably to the adsorption characteristics of a commercially available activated alumina.

The laboratory test proceeded as follows. A small sample of low density sorbent was dried by heating and weighed. The sample was then placed into a glass reactor, heated, and fluidized by a nitrogen stream containing a known amount of water. In order to simulate the POC adsorber, the bed temperature was 250°F, the gas residence time was 1 second and the sorbent residence time was 45 minutes. Tests were run at stream water contents of 3%, 5%, and 7%. At the end of each test, the sorbent sample was reweighed in order to establish the weight gain due to water adsorption. The system pressure was also recorded in order to evaluate the stream dew points for the purpose of comparing the results to other alumina based beads.

The results of this test are presented in Figure 3-11. Also shown is the isotherm for commercially available activated alumina, used in desiccant applications. This alumina has a surface area of 355 m^2/g, thus a surface area correction factor was applied to its isotherm for comparison to the lab results, which used NOXSO sorbent with a surface area of 155 m^2/g. As shown in the graph, NOXSO low density sorbent compares very well to the surface area corrected alumina.

Finally, use of the lab results and the commercial isotherms has satisfied the energy balance closures of the POC. By using the surface area corrected isotherms, the energy balance closures of the sorbent heater and sorbent cooler now satisfy the tolerances established by the previously reported uncertainty analysis. For this reason, the isotherms with surface area correction are used in the NOXSO computer simulation program.

3.5.5 Fluid Bed Gas Flow Modeling

In order to provide information for the design of fluid bed vessels, fluid bed gas flow modeling has been performed using a computational fluid dynamics (CFD) software package - PHOENICS. The gas phase governing equations are solved using the finite volume method with specified boundary conditions. The k-ϵ turbulence model is used to simulate the flow turbulence. The numerical simulation can give distributions of the velocity, temperature, pressure, etc. in the whole flow field. The results can be analyzed for the guidance of the vessel design.

The gas flows from the top bed of the sorbent heater were modeled for the proof-of-concept (POC) plant and commercial plant. Since the POC was already built and tested, its numerical simulation combined with test results can be used for the purpose of evaluation of the computer code. The numerical data was also compared with the analytical data. Due to the nature of asymmetric flow, only half of the vessel was simulated. The geometric and physical conditions are given in Table 3-5.

Figure 3-11. NOXSO Sorbent Water Adsorption Isotherm

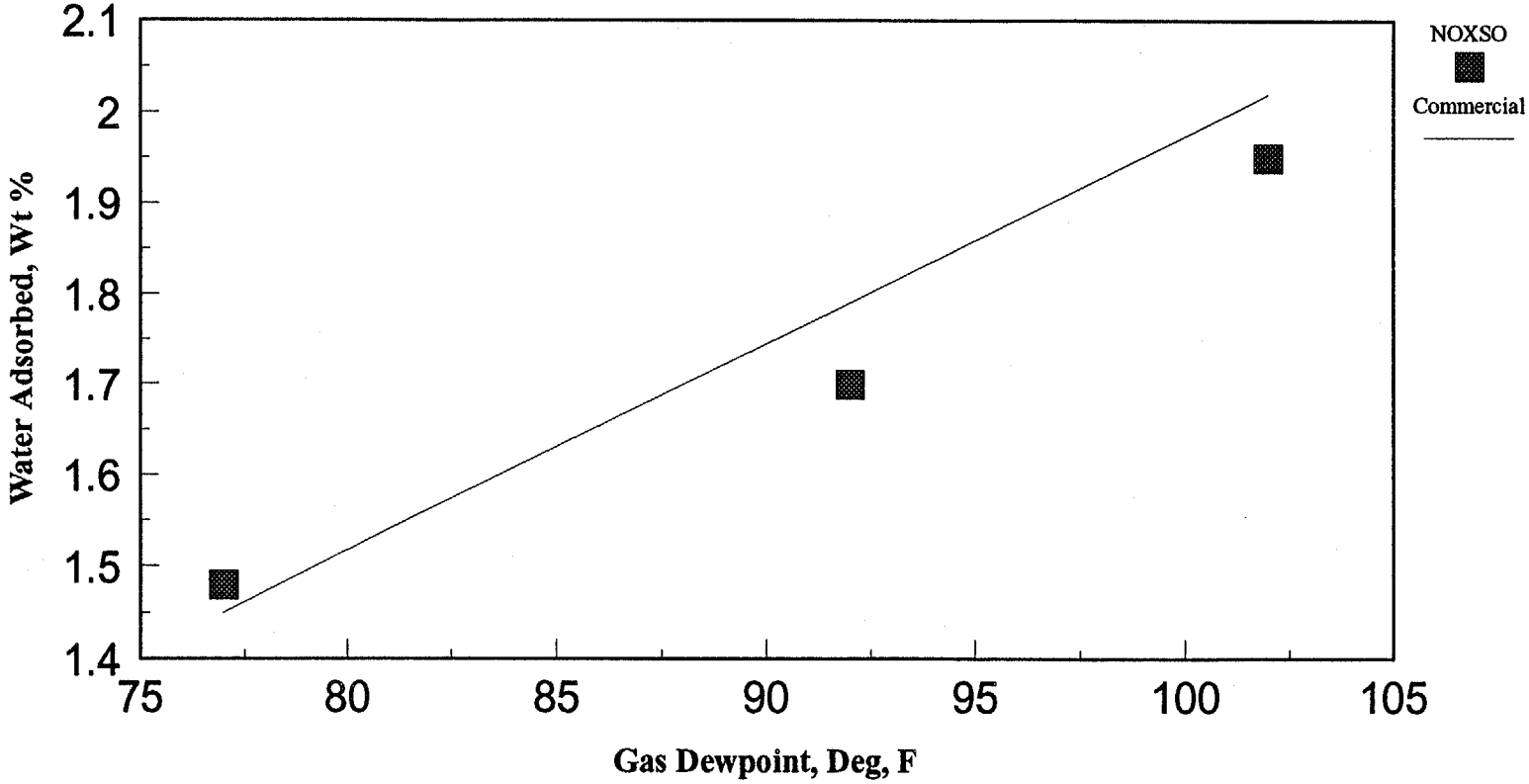

Bed Temperature = 250 deg F

Surface Area Correction = 155/355

Table 3-5. Geometric and Physical Conditions		
	POC	Commercial
Vessel Radius	1.17 m	4.42 m
Nozzle Radius	0.254 m	1.07 m
Top Grid to Nozzle Distance	2.00 m	4.51 m
Nozzle Length	0.508 m	2.13 m
Head Shape	Torispherical	2:1 elliptical
Inlet Velocity	0.820 m/s	0.910 m/s
Temperature	343 °C	260 °C
Settled Bed Height	30.5 cm	30.5 cm

Figure 3-12 shows the streamlines of gas flow for the sorbent heater of the commercial plant. Figure 3-13 displays the axial velocity contours with each line representing a constant velocity. The gas flow is uniformly distributed at the bottom, and then accelerates due to the reduced flow area.

Figure 3-14 shows the profile of axial velocity at the nozzle exit for the POC plant with a comparison between numerical data and analytical data. The analytical data was obtained from the classic expression of fully developed turbulent flow in a circular tube ("Transport Phenomena" by R. Byron, etc., John Wiley & Sons, 1960). The numerical results showed reasonable agreement with the analytical results.

Figure 3-15 displays the axial velocity distributions along the centerline of the sorbent heater. The velocity remains unchanged to a certain distance above the grid, and then accelerates to another constant velocity inside the nozzle. This information is useful for the vessel design. In general, the top bed can be divided into two zones - the uniform velocity zone and acceleration zone. From the design point of view, for a given superficial velocity, the height of the uniform velocity zone should be equal to the transport disengaging height (TDH), so that no significant carryover of sorbent occurs. The TDH at given conditions was experimentally investigated in the NOXSO laboratory previously. The test facility was a 2 ft x 2 ft cold flow model. The sorbent entrainment versus the distance above the gas distributor is plotted in Figure 3-16. The TDH is the distance above the gas distributor beyond which sorbent entrainment remains constant. Applying Figure 3-16, for the POC sorbent heater operating conditions, the TDH is estimated at 1.2 m (4 ft). From numerical results as shown in Figure 3-15, the uniform velocity zone is approximately 1.1 m high, which is very close to the estimated TDH and indicates that the design of the POC sorbent heater is reasonable. During POC operation, no significant sorbent carry over was observed. The agreement between the numerical results and the test results indicates that the numerical simulation is reliable. Therefore, the same approach can be applied to the design of commercial vessels. From the

Figure 3-12. Streamlines of Gas Flow in Sorbent Heater

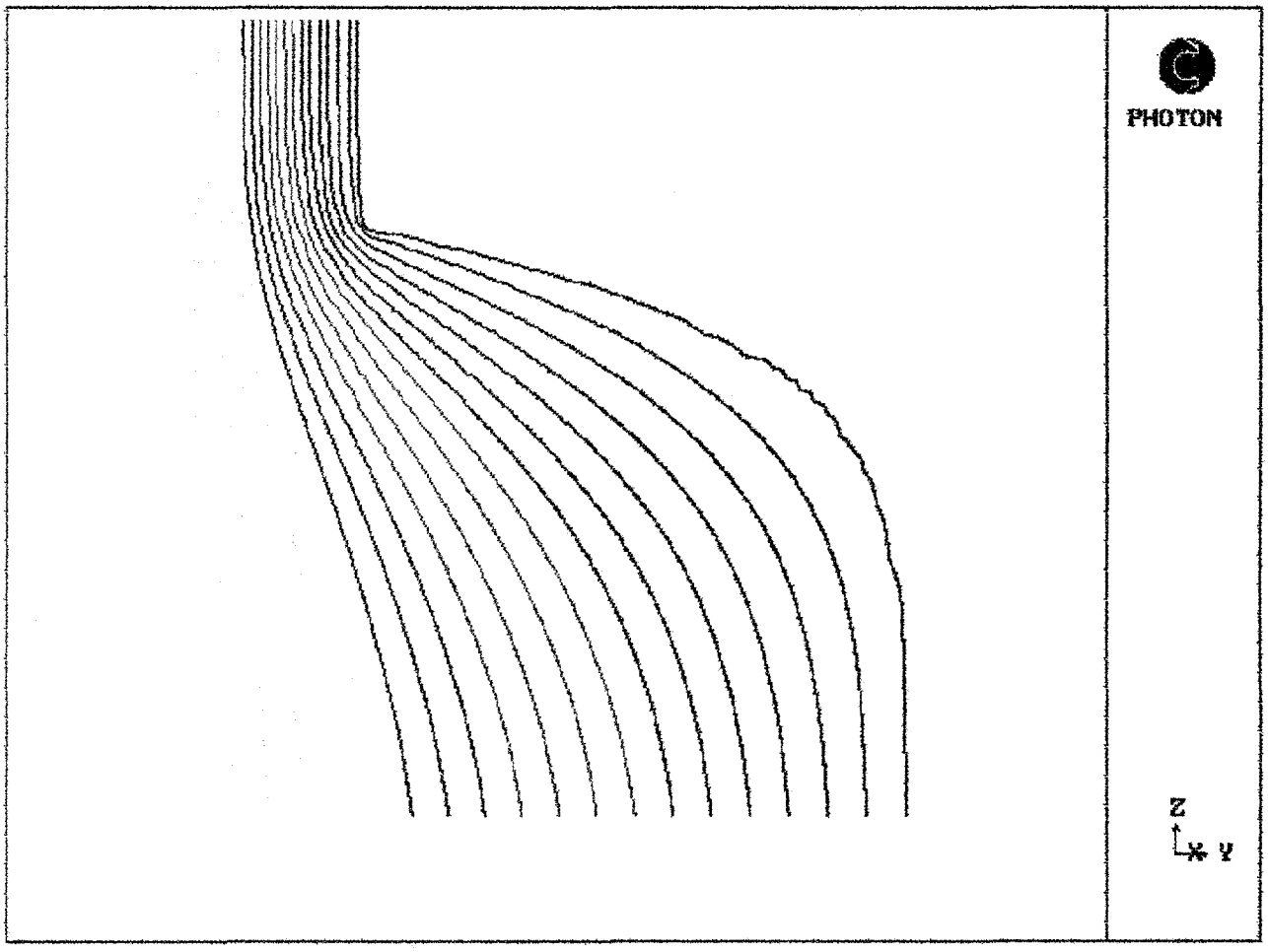

Figure 3-13. Axial Velocity Contours of Gas Flow in Sorbent Heater

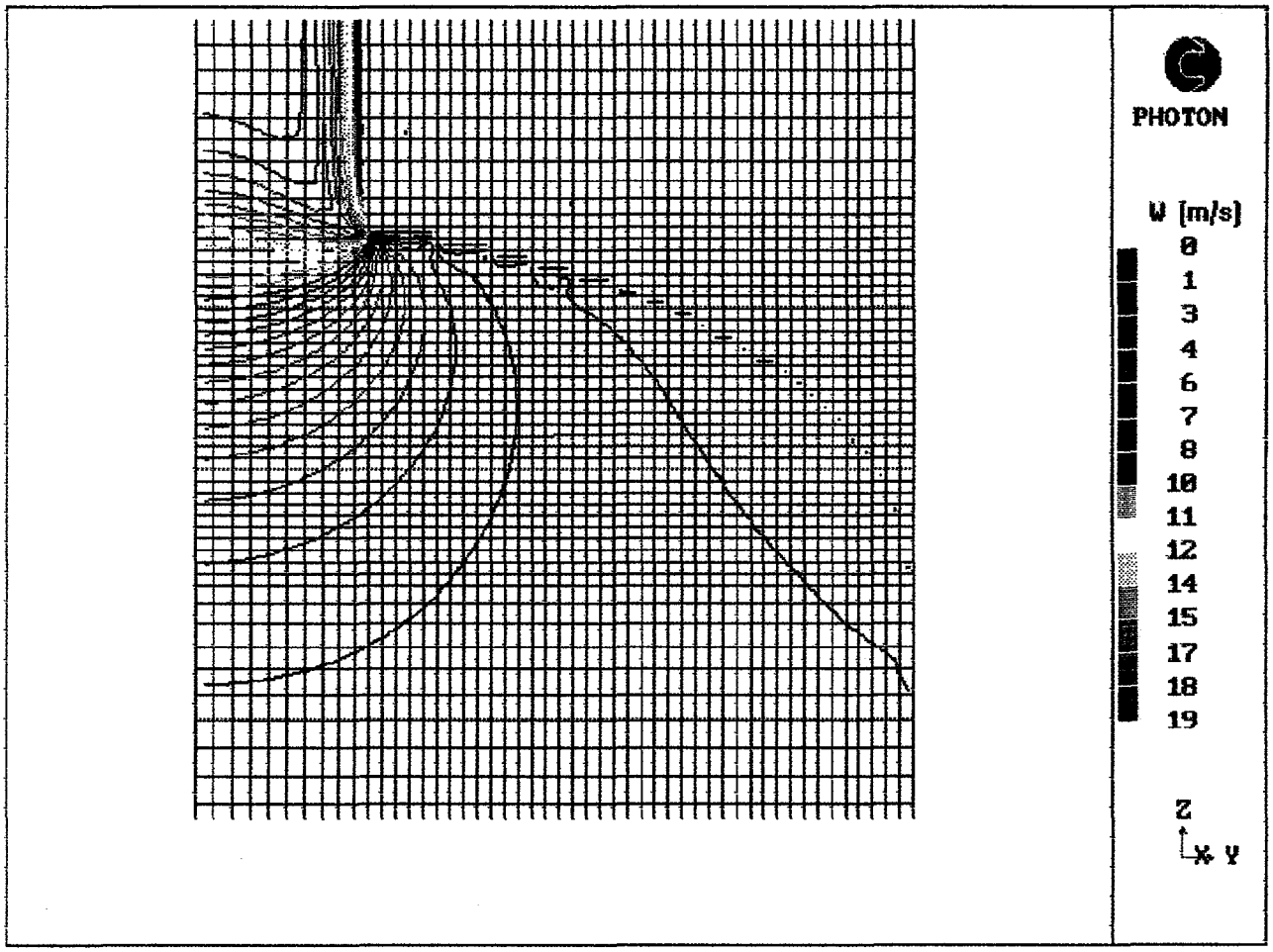

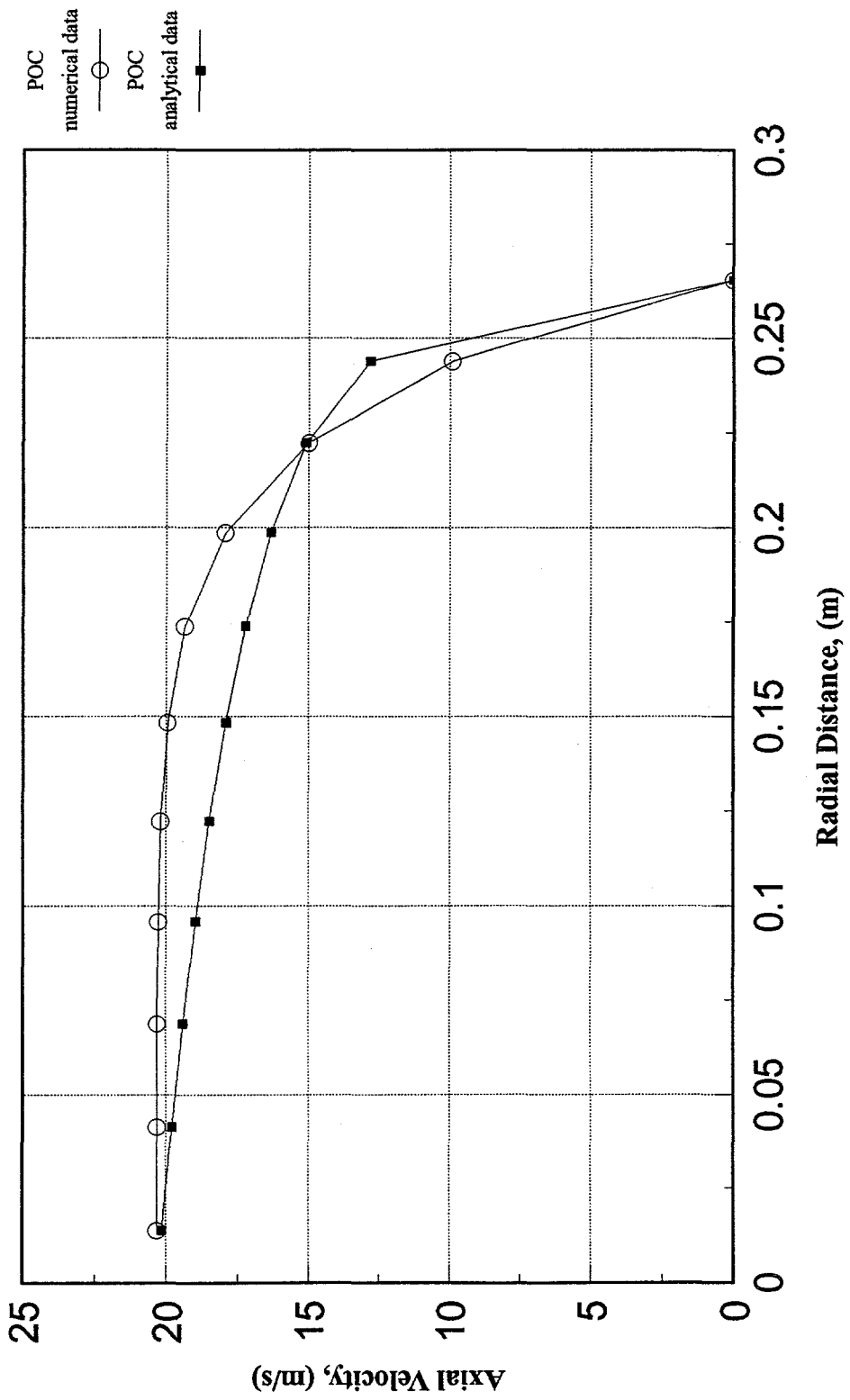

Figure 3-14. Exit Nozzle Axial Velocity Profile

Figure 3-15. Sorbent Heater Top Bed Centerline Axial Velocity

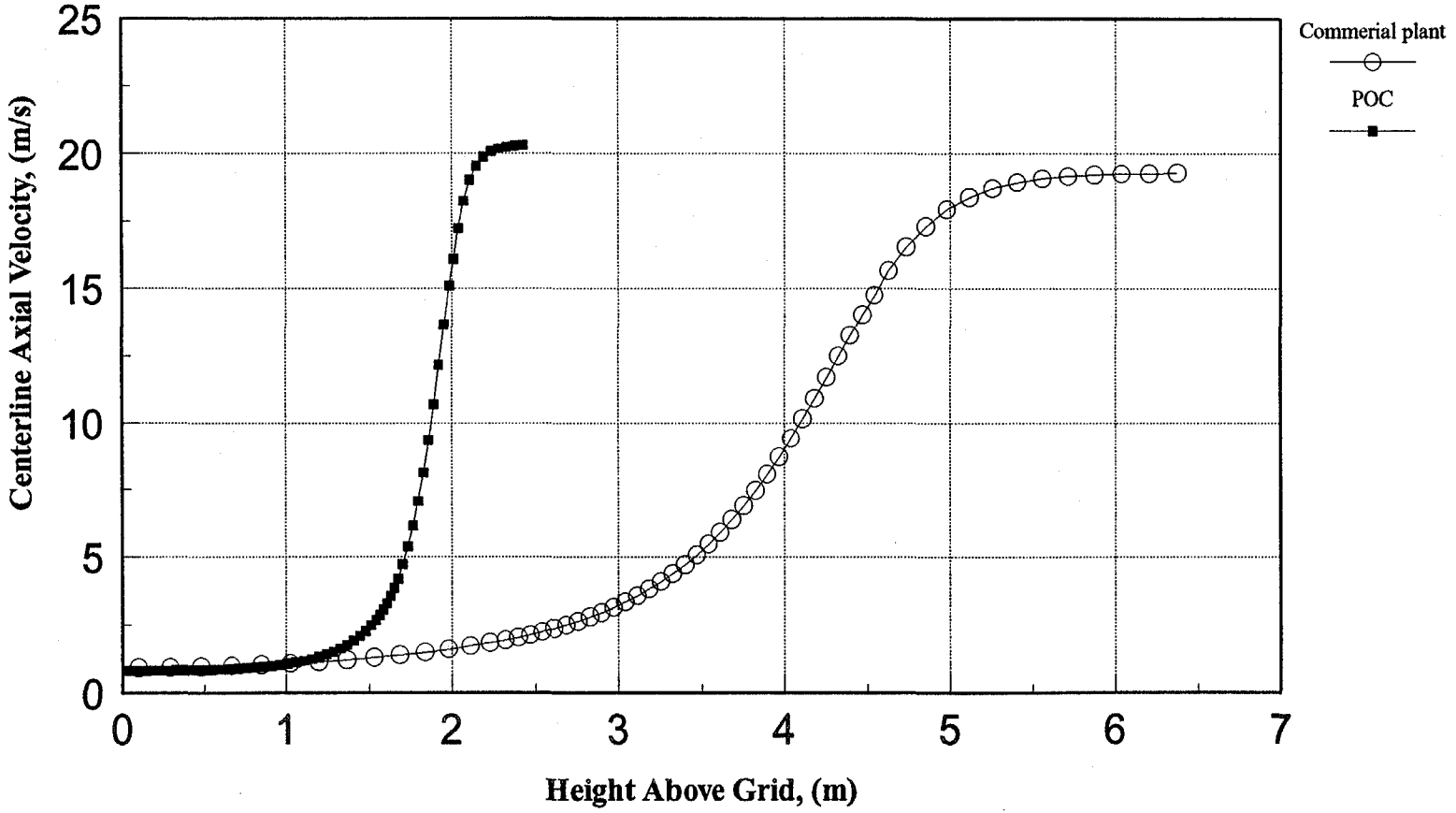

Figure 3-16. Sorbent Entrainment Versus Height Above Distributer

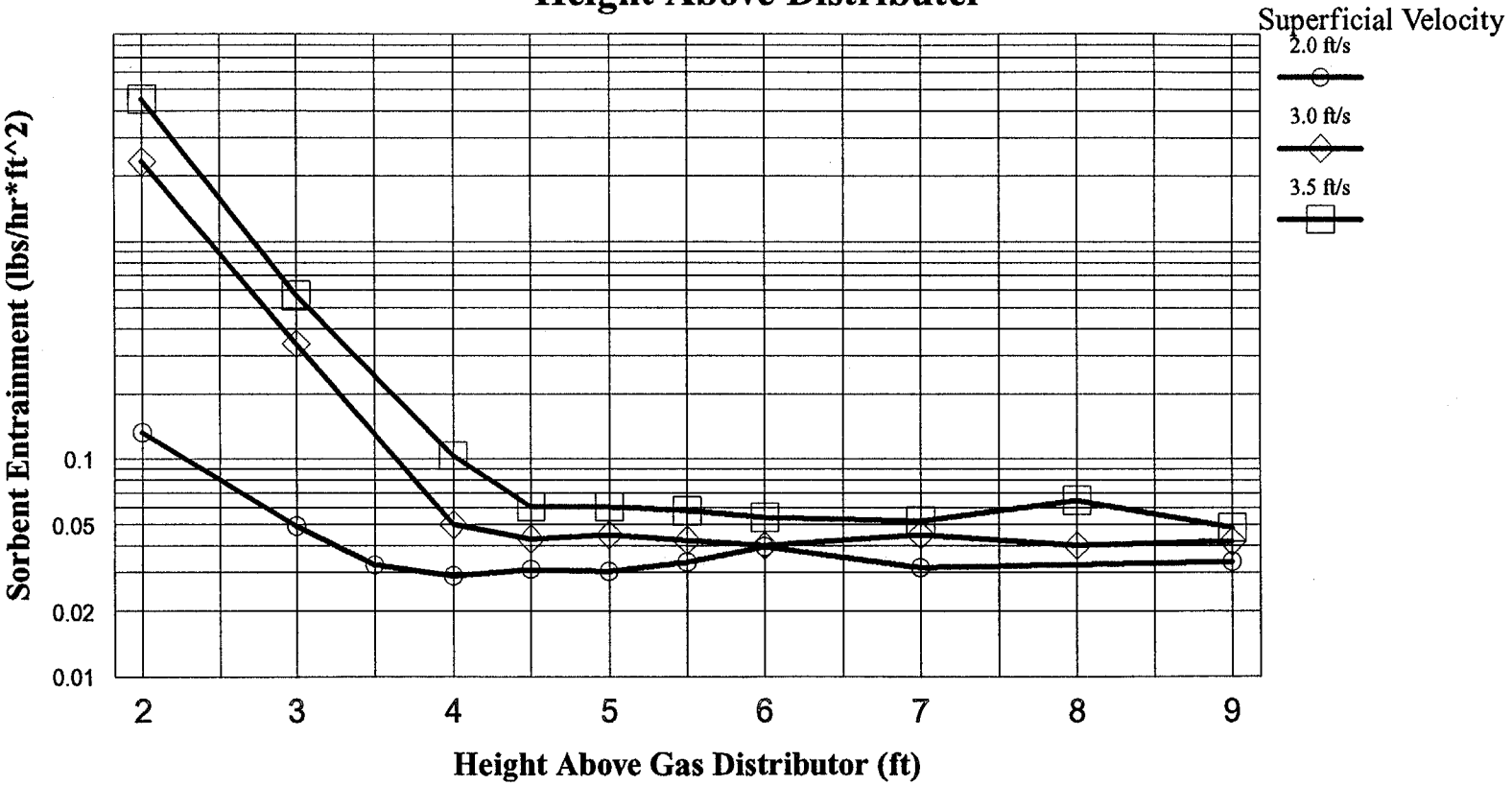

2-ft x 2-ft Cold Flow Model

12-in Settled Bed Depth

numerical results as shown in Figure 3-15, the uniform velocity zone for the top bed of the sorbent heater for the commercial plant is approximately 1.5 m, which is a little larger than the TDH. This also indicates that the design of the commercial sorbent heater is reasonable. A small reduction in vessel height may be possible, which will be investigated in future numerical studies.

3.6 Plant Characterization

Plant characterization activities are on hold until a new host site is identified.

3.7 Site Survey/Geotechnical Investigation

Site survey/geotechnical investigation activities are on hold until a new host site is identified.

3.8 Permitting

Permitting activities are on hold until a new host site is identified.

4 PLANS FOR NEXT QUARTER

The main priority for the next quarter is the evaluation and selection of a host site for the project. It is essential that a technically acceptable host site be selected so the process can be properly demonstrated.

Immediately upon selection of the host site, work will begin to modify the EIV with information specific to the new site. It is critical to satisfy the NEPA requirements as soon as possible to prevent this from delaying the project.

Mechanical design options for the process vessels will continue to be evaluated with particular focus on the sorbent heater. The tests to verify performance of the flue gas particulate separator will be conducted.

Equipment and samples from the POC which were examined and collected will be evaluated with regard to erosion and corrosion characteristics. Results of this study will be summarized.

The regenerator computer model will be used to determine reaction rate constants based on laboratory data. The model predictions will then be compared with data collected during operation of the POC.

Fluid bed computer modeling will be used to assure that an adequate acceleration zone is provided in all fluid bed vessels and that grid pressure drops are high enough to assure uniform gas distribution across the vessel.